Food Packaging and Shelf Life 21 (2019) 100365

Contents lists available at ScienceDirect

Food Packaging and Shelf Life

journal homepage: www.elsevier.com/locate/fpsl

Natural plant extracts as active components in chitosan-based films: A comparative study

Marijan Bajić[a,*], Tina Ročnik[a], Ana Oberlintner[a], Francesca Scognamiglio[b], Uroš Novak[a], Blaž Likozar[a]

[a] Department of Catalysis and Chemical Reaction Engineering, National Institute of Chemistry, Hajdrihova 19, 1000 Ljubljana, Slovenia
[b] Department of Life Sciences, University of Trieste, Via Licio Giorgieri 5, 34127 Trieste, Italy

ARTICLE INFO

Keywords:
Chitosan-based material film
Natural plant extract
Active food packaging
Structural and mechanical characterization
Total phenolic content
Antibacterial activity

ABSTRACT

Chitosan-based films with separately incorporated plant extracts obtained from oak (*Quercus robur*), hop (*Humulus lupulus*), and brown algae (*Laminaria hyperborea*) were evaluated and mutually compared regarding structural, physicochemical, and antibacterial properties. Processing of chitosan and extracted raw substances led to the development of blended films with diverse physical appearances and physicochemical properties. Starting from the oak extract-containing film and ending with the algal extract-containing film, blended films shown ascending trends in moisture content (21.5% – 28.3%), total soluble matter (23.8% – 28.9%), and elongation at break (14.0% – 31.0%) as well as descending trends in tensile strength (12.7 MPa – 5.5 MPa), Young's modulus (230.8 MPa – 19.4 MPa), and total phenolic content (9.1 $mg_{GAE}\ g_{film}^{-1}$ – 1.0 $mg_{GAE}\ g_{film}^{-1}$). The films loaded with oak and hop extracts had improved optical properties reflected in the ability to completely block the light transmittance at the wavelengths below ~330 nm. Moreover, the same films exhibited the appearance of inhibition zones implying the antibacterial activity against *Bacillus subtilis*.

1. Introduction

Cationic polysaccharide chitosan is a deacetylated derivative of chitin – an abundantly present and renewable biopolymer that is mostly obtained from marine sources (Borić, Puliyalil, Novak, & Likozar, 2018; Younes & Rinaudo, 2015). Chitosan has been extensively studied for potential applications in biomedical, biotechnological, pharmaceutical, and food sectors due to its prominent characteristics such as non-toxicity, biodegradability, biocompatibility as well as inherent antimicrobial activity and good film-forming capability (Hosseinnejad & Jafari, 2016; Muxika, Etxabide, Uranga, Guerrero, & de la Caba, 2017; Younes & Rinaudo, 2015). One of the most promising applications of chitosan is the preparation of chitosan-based films and coatings, which have emerged as an effective and eco-friendly way to extend the shelf life of perishable foods (Elsabee & Abdou, 2013).

Chitosan-based films, which are commonly prepared by means of casting method followed by drying at moderate temperatures, might be a sustainable alternative to eco-unfriendly synthetic plastics (Homez-Jara et al., 2018; Leceta, Guerrero, Cabezudo, & de la Caba, 2013). They can also be used as active food packagings after the incorporation of various components capable of enhancing the antioxidant and/or antimicrobial properties and therefore protective capacity (Lunkov, Ilyina, & Varlamov, 2018; Mujtaba et al., 2019; Yuan, Chen, & Li, 2016). So far, numerous plant extracts have been studied regarding their effects on techno-functional characteristics of the packaging films intended for food protection (Mir, Dar, Wani, & Shah, 2018). Some of the most recent studies are scrutinizing chitosan-based films with incorporated plant extracts, including *Camelina sativa* seed oil (Gursoy et al., 2018), *Pistacia terebinthus* stem, leaf and seed extracts (Kaya, Khadem et al., 2018), *Berberis crataegina* fruit extract and seed oil (Kaya, Ravikumar et al., 2018), *Prunus armeniaca* kernel essential oil (Priyadarshi et al., 2018), *Eucalyptus globulus* essential oil (Hafsa et al., 2016), tea extracts (Siripatrawan & Harte, 2010; Wang, Dong, Men, Tong, & Zhou, 2013), algal extract from *Codium tomentosum* (Augusto et al., 2018), and many others (Genskowsky et al., 2015; Kalaycıoğlu, Torlak, Akın-Evingür, Özen, & Erim, 2017; Peng, Wu, & Li, 2013; Serrano-León et al., 2018; Souza et al., 2017; Sun et al., 2017).

Our previous study has already shown that a supercritical CO_2 hop extract is very suitable to be used as the active (antioxidant and/or antimicrobial) component in chitosan-based films (Bajić, Jalšovec, Travan, Novak, & Likozar, 2019). Still, there are many plant extracts to be addressed for the same purpose. For instance, the heartwood of the oak tree

* Corresponding author.
E-mail address: marijan.bajic@ki.si (M. Bajić).

https://doi.org/10.1016/j.fpsl.2019.100365
Received 10 January 2019; Received in revised form 29 May 2019; Accepted 7 July 2019
Available online 20 July 2019

is rich in ellagitannins, mostly castalagin and vescalagin (García-Estévez, Alcalde-Eon, Le Grottaglie, Rivas-Gonzalo, & Escribano-Bailón, 2015; de Simón, Cadahía, Conde, & García-Vallejo, 1999). Consequently, oak extracts possess antimicrobial and antioxidant activity that contributes to a shelf life extension of perishable foods (Soriano et al., 2018). Besides terrestrial plants, brown algae present another renewable source of the active compounds, such as phlorotannins (Li, Wijesekara, Li, & Kim, 2011). Hence, crude extracts obtained from brown algae (Balboa, Conde, Moure, Falqué, & Domínguez, 2013), including that obtained from the species *Laminaria hyperborea* (O'Sullivan et al., 2011), should be considered as abundantly present and relatively cheap active components suitable for the incorporation into chitosan-based films.

The aim of this study was to test and mutually compare three different plant extracts (oak, hop, and algal) as the active components in chitosan-based films. Therefore, three different extract-containing chitosan-based films were prepared and further evaluated regarding the effect of extracts incorporation on their structural, physicochemical, and antimicrobial properties.

2. Material and methods

2.1. Material

High molecular weight chitosan (310–375 kDa; ≥75% deacetylated), lactic acid (≥85%), Folin-Ciocalteu´s phenol reagent, and gallic acid were from Sigma-Aldrich (Steinheim, Germany). Sodium carbonate, glycerol, and absolute ethanol were from Merck (Darmstadt, Germany), Pharmachem Sušnik (Ljubljana, Slovenia), and Honeywell (Hannover, Germany), respectively. Excluding lactic acid, all chemicals were of analytical grade. Milli-Q® water was used throughout all experiments.

2.2. Plant extracts and preparation of film-forming solutions/chitosan-based films

2.2.1. Plant extracts

The oak extract, obtained from the extra selected parts of Slavonian oak (QuerTan; Tanin, Sevnica, Slovenia), was added in the film-forming solution in powder form (Section 2.2.2).

A commercially available hop extract (a viscous semi-fluid substance under ambient conditions) was firstly placed in a small glass beaker, and then heated under a jet of warm tap water in order to lower its viscosity, as previously described (Bajić et al., 2019). Afterwards, it was transferred to a plastic syringe and eventually added dropwise into the chitosan solution (Section 2.2.2).

A crude algal extract was prepared by adding 1 g of grounded algae stipes (collected from the coastal area of Norway in September 2018) in 10 mL of water followed by mixing at room temperature for 24 h, separation through a syringe filter Chromafil® Xtra CA-20/13 with pore size 0.22 µm (Macherey-Nagel, Düren, Germany), and drying in the oven with continuous ventilation Kambič SP-55 C (Kambič, Semič, Slovenia) at 40 °C until constant mass. Obtained extract powder was added in the chitosan solution as described in Section 2.2.2.

2.2.2. Preparation of film-forming solutions/chitosan-based films

Chitosan solution was prepared according to a slightly modified protocol explained elsewhere in the literature (Bajić et al., 2019). Shortly, 1.5% (w/v) of chitosan and 30.0% (w/w) of glycerol (plasticizer; calculated based on the mass of chitosan) were dissolved in a 100 mL of 1.0% (v/v) aqueous solution of lactic acid and the mixture was continuously stirred overnight on a magnetic stirrer IKA® RCT (IKA, Staufen, Germany) at 1000 rpm and room temperature (24 °C).

Since the extraction yield of algal extract is relatively low at the lab scale (and besides the film-forming solutions with higher concentrations of the oak extract become viscous and difficult to filtrate), each plant extract was separately added in a 100 mL of chitosan solution at the level of 0.1% (w/v) in order to enable comparison between the samples. The mixtures were then homogenized on Ultra-Turrax® T50 homogenizer (IKA, Staufen, Germany) at 6000 rpm during 2 min, and vacuum-filtered through two sheets of medical gauze to get rid of the retained impurities.

Prepared film-forming solutions were cast in polyurethane Petri dishes (~0.32 mL cm^{-2}) and left in drying oven at 40 °C for the next 48 h. Obtained films were peeled off from the Petri dishes eventually, and stored under ambient conditions (room temperature; relative humidity, RH ~45-55%; restricted exposure to sunlight) until further analysis.

The samples are labelled with the letters indicating either the control film prepared without any extract (CH) or the films with incorporated oak extract (OE), hop extract (HE), and algal extract (AE).

2.3. Morphological properties and thickness

Surface and cross-section morphology of chitosan-based films was studied by means of the scanning electron microscopy (SEM) performed by SUPRA 35VP electron microscope (Carl Zeiss, Jena, Germany).

Film thicknesses were determined from the SEM pictures of the films' cross-sections, whereby the distances between opposite edges of the films were measured at ten different places using the image analysis software ImageJ (National Institutes of Health, Bethesda, USA), and the results were averaged. The method was confirmed by measuring the film thicknesses using ABS Digital Thickness Gauge (Mitutoyo, Aurora, USA) (Bajić et al., 2019).

2.4. Fourier-transform infrared spectroscopy analysis

The Fourier-transform infrared (FT-IR) spectra of chitosan powder, plant extracts, and obtained films were recorded at the wavenumbers ranging from 4000 cm^{-1} to 400 cm^{-1} and resolution 4 cm^{-1}. The measurements were performed at room temperature using Spectrum Two FT-IR spectrometer (PerkinElmer, Waltham, USA). The resulting spectra (Section 3.2) present the average of three independent measurements.

2.5. Moisture content and total soluble matter

Moisture content (*MC*) and total soluble matter (*TSM*) were determined gravimetrically (Bajić et al., 2019). Briefly, the samples were cut into rectangular pieces (~1 cm^2), weighted on analytical balance (Kern & Sohn, Balingen, Germany) in order to get the initial mass (M_1), and then dried in drying oven at 105 °C for 24 h to get the initial dry mass (M_2). The oven-dried samples were then dipped in the sealed glass vials containing 30 mL of water and kept at room temperature for 24 h. Thereafter, the samples were removed from the vials and dried again at 105 °C for 24 h to get the final dry mass (M_3).

MC $[(M_1 - M_2 / M_1) \times 100\%]$ presents the percentage of water content in the films after drying at above-defined conditions, while *TSM* $[(M_2 - M_3 / M_2) \times 100\%]$ presents the percentage of the total dry matter that is soluble in water after the film immersion for 24 h (Bajić et al., 2019).

2.6. Optical transmittance

Optical properties of chitosan-based films were evaluated in terms of the light transmittance in the UV–vis region (Bajić et al., 2019). Rectangular film samples were placed in a cuvette and the absorbance (A) was recorded on Lambda 40 UV/Vis spectrophotometer (PerkinElmer, Waltham, USA) under the wavelengths region ranging from 250 nm to 800 nm. The measurements were performed at room temperature, and the results were expressed as percent transmittance (%T) of the samples, following that $\%T = 10^{-A} \times 100$. An empty cuvette (i.e. air) was used as the reference.

2.7. Mechanical properties

Mechanical properties were studied using the universal testing machine Multitest 2.5-i (Mecmesin, Slinfold, UK) equipped with a 100 N load cell. The tests on the rectangular film samples (length × width : 8 cm × 2 cm) were performed at a crosshead speed of 5 mm min^{-1}, following the ASTM D 882 standard method (2002) with slight modifications. Tensile strength (*TS*) was calculated by dividing the load with the average original cross-sectional area in the gage length segment of the sample (6 cm), elongation at break (*EB*) was calculated as the ratio between increased length after breakage and the initial gage length, while Young's modulus (*YM*) was calculated as the slope of the linear portion in the stress-strain curve, considering deformation range of 1–3% (Bajić et al., 2019).

2.8. Total phenolic content

An approximate assessment of the total phenolic content (*TPC*) in chitosan-based films was determined using Folin-Ciocalteu's (FC) phenol reagent. In short, small rectangular film samples were added in water (~5 mg of the film per mL of water), followed by successive addition of the FC phenol reagent and 10% (w/v) aqueous solution of Na_2CO_3 in the amounts of 10 vol% and 20 vol% based on the volume of water, respectively. The samples were incubated for 2 h in a dark place at room temperature, and the absorbance was measured at 765 nm using Synergy™ 2 Multi-Detection Microplate Reader (BioTek, Winooski, USA). Gallic acid was used as the standard and the results were expressed as the mass of gallic acid equivalent (GAE) per mass of films.

2.9. Antibacterial properties

Two bacterial species, namely Gram-negative *Escherichia coli* K12 (*E. coli*) and Gram-positive *Bacillus subtilis* DSM 402 (*B. subtilis*) were used for the assessment of the antibacterial activity of chitosan-based films. A 100 μL of freshly prepared bacterial culture suspension in the exponential growth phase (with the OD_{600} value set to 0.5) was spread over the Luria-Bertani agar culture medium, and the UV light-sterilised (at 254 nm for 15 min; both sides) rectangular film samples (~1 cm^2) were placed on the plate surfaces and incubated at 37 °C for 24 h (Bajić et al., 2019). The appearance of a clear area below the films was marked as the contact inhibition, while the clear zones around the films were recorded as the inhibition zones.

2.10. Statistical analysis

Statistical analysis was done using the one-way ANOVA with the confidence level of 95% ($p < 0.05$) in conjunction with Tukey's honestly significant difference post-hoc test. All experiments were done in triplicates and the results were expressed as the mean ± standard deviation.

3. Results and discussion

3.1. Morphological properties and thickness

Upon the addition of extracts in a viscous and transparent chitosan solution and subsequent homogenization of the mixtures, a series of film-forming solutions with different color shades spanning from a pale-brownish (OE), over a pale-yellowish (HE), to white (AE) was obtained (Fig. 1; columns A and B).

Using the film-forming solutions presented in Fig. 1 (column B), compact, smooth, homogeneous, and mechanically stable chitosan-based films without (control film) or with incorporated plant extracts (blended films), were prepared (Fig. 1; column C). The samples were plane and their edges did not exhibit rolling over to the inside. Visual appearance was similar since all films were glossy and transparent, with an exception regarding the color shade that was nonexistent, a pale-brownish, and a pale-yellowish for CH/AE, OE, and HE films, respectively (Fig. 1; column C).

The SEM analysis was performed in order to visualize the surfaces and cross-sections of chitosan-based films. The analysis has revealed that all samples had relatively smooth and uniform surfaces, without any drastic difference between the control and blended films (Fig. 1, column D). Similarly, all samples were compact and without any visible cracks or pores at the cross-sections (Fig. 1, column E). The average thicknesses of 43 ± 1 μm, 53 ± 2 μm, 59 ± 1 μm, and 36 ± 1 μm were determined for CH, OE, HE, and AE films, respectively (Fig. 1, column E). The values are similar to those reported for the other chitosan-based films with incorporated extracts (Souza et al., 2017).

3.2. Fourier-transform infrared spectroscopy analysis

In order to detect the absorption intensity of the most specific functional groups in chitosan powder and plant extracts, FT-IR analysis was carried out and the resulting spectra can be seen in Fig. 2a. By its structure, the chitosan molecule is a linear copolymer of D-glucosamine and *N*-acetyl-D-glucosamine (Muxika et al., 2017), while the most prevalent components in the oak, hop, and algal extracts are expected to be ellagitannins (de Simón et al., 1999; García-Estévez et al., 2015), α-acids/β-acids (Bajić et al., 2019), and phlorotannins (Li et al., 2011), respectively (in addition, chromatograms of commercial tannic acid standard (Fig. S1), hop extract (Fig. S2), and algal extract (Fig. S3) can be seen in Appendix A).

The used extracts are quite complex and dissimilar in their composition, but if the FT-IR spectra from Fig. 2a are evaluated in terms of the most prevalent components, some general conclusions can be made. Namely, all above-listed components contain a relatively high number of O–H and C=O functional groups. Therefore, the broad absorption bands in the region between 3600 cm^{-1} and 3100 cm^{-1} are likely corresponding to O–H (and N–H in case of chitosan) bond stretching, the absorption bands recorded in the region between 3000 cm^{-1} and 2800 cm^{-1} to C–H bond stretching, while the absorption peaks recorded in the region between 1750 cm^{-1} and 1500 cm^{-1} are corresponding to C=O bond stretching (Fig. 2a) (Talari, Martinez, Movasaghi, Rehman, & Rehman, 2017). Other significant peaks related to chitosan powder/chitosan-based films detected between 1650 cm^{-1} and 950 cm^{-1} in the spectra of chitosan powder (black dash-dotted line in Fig. 2a) and/or chitosan-based films (black solid line in Fig. 2b) are considered to be corresponding to N–H bending, C–N stretching, and C–O stretching (Bajić et al., 2019).

After the film formation, the most notable structural modifications observed by comparing the spectra of chitosan powder (Fig. 2a) and CH film (Fig. 2b) might be ascribed to the interactions between chitosan, plasticizer (glycerol), lactic acid, and water (Bajić et al., 2019 and ref. therein). Moreover, the incorporation of plant extracts caused additional changes which are evident from the spectra of OE, HE, and AE films. Namely, the broad absorption band corresponding to O–H stretching vibrations and the peaks corresponding to C=O stretching and N–H bending have increased in intensity in regard to the spectrum of CH control (Fig. 2b). On this basis, it can be discussed that chitosan molecules establish intra- and intermolecular hydrogen bonds over their O–H and N–H functional groups. The intermolecular hydrogen bonds are in all probability formed between O–H and N–H groups of chitosan molecule and O–H groups of the most prevalent components from the plant extracts, as proposed in the study by Bi et al. (2019). Besides, C=O functional groups from chitosan (acetylated monomers) and plant extracts' components can be involved in the hydrogen bond-based interactions as well (Akyuz et al., 2018; Kaya, Khadem et al., 2018), but presumably in smaller extent than O–H groups since their number is generally smaller. The exceptions are hop extract's components which possess two C=O groups versus three (α-acids) and two (β-

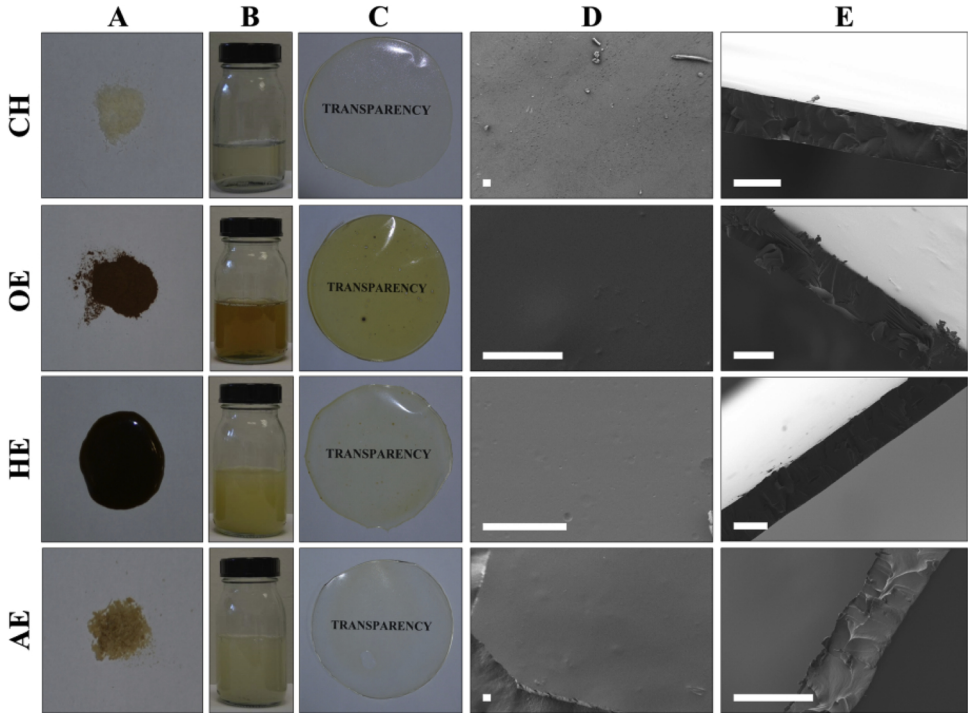

Fig. 1. Physical appearance of raw materials, film-forming solutions, and chitosan-based films: (A) chitosan powder and plant extracts; (B) chitosan solution and film-forming mixtures containing plant extracts; (C) macroscopic appearance of chitosan-based films; (D) microscopic appearance of chitosan-based films' surfaces (SEM images); (E) microscopic appearance of chitosan-based films' cross-sections (SEM images). Scale bars in (D) and (E) indicate the length of 50 μm.

acids) O–H groups (Bajić et al., 2019).

3.3. Moisture content and total soluble matter

The amount of bound water, which mostly depends on the film composition as well as temperature and time of drying, can significantly influence the physical properties of chitosan-based films (Homez-Jara et al., 2018). This particularly refers to the ability of material to prevent/reduce moisture transfer between food and its surroundings because the presence of water molecules within the film matrix leads to the formation of amorphous zones, and therefore different internal structural rearrangement which allows water permeation (Aguirre-Loredo, Rodríguez-Hernández, Morales-Sánchez, Gómez-Aldapa, & Velazquez, 2016; Homez-Jara et al., 2018).

As evident from Table 1, all blended films had smaller values of *MC* then the control sample. More accurately, the AE film had a slightly smaller value, while the values significantly decreased after the incorporation of oak and hop extracts. Namely, the hydrogen bonding interactions that occur between chitosan molecules and the most prevalent components of the plant extracts (Section 3.2) could be competitive with chitosan-water hydrogen bonding (Bajić et al., 2019; Peng et al., 2013; Sun et al., 2017), which might be the reason for lower *MC* in blended films.

Table 1
Moisture content and total soluble matter in chitosan-based films.

Film sample	*MC [%]	*TSM [%]
CH	29.6 ± 0.9[a]	23.5 ± 0.6[a]
OE	21.5 ± 0.9[b]	23.8 ± 0.2[a]
HE	23.6 ± 0.1[b]	25.3 ± 0.8[a]
AE	28.3 ± 0.9[a]	28.9 ± 0.4[b]

* The samples with different letters have significantly different mean values ($p < 0.05$).

TSM is a very important characteristic referring to the biodegradability of chitosan-based films (Peng et al., 2013). However, it should be minimal when material integrity and water-resistance are required (Gursoy et al., 2018; Hafsa et al., 2016), otherwise, it would negatively

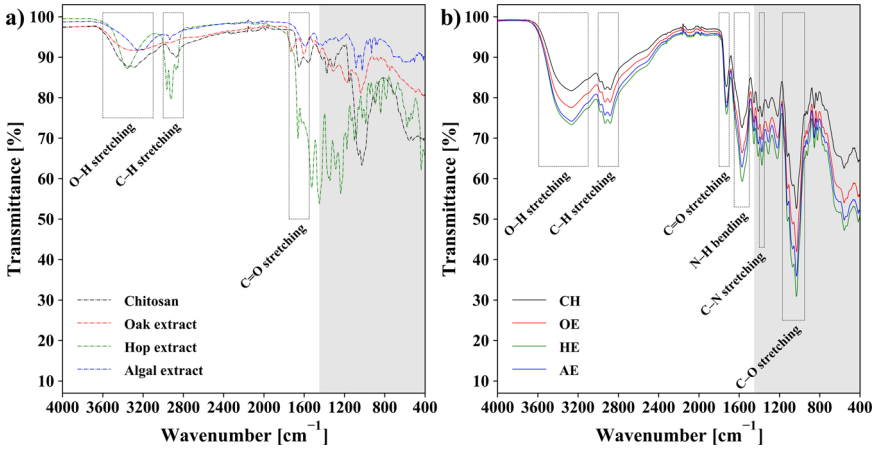

Fig. 2. FT-IR spectra of: a) raw materials (chitosan powder and plant extracts); b) chitosan-based films. The grey-shaded area represents the fingerprint region. The dashed rectangles are only for visual guidance.

affect the protection of the food with high moisture content.

The incorporation of oak and hop extracts did not significantly affect *TSM* in regard to the control film (Table 1). Such results could be a consequence of relatively small amount of incorporated extracts, which is basically not able to alter *TSM* remarkably. Only the AE film had significantly higher *TSM* relative to other films, which was somehow expected because the used algal extract was a water-based one (Section 2.2.1). Anyway, the entire *TSM* value range is in accordance with the value range reported for other chitosan-based films containing either oil-based or water-based natural antioxidants (Souza et al., 2017).

3.4. Optical transmittance

The characteristics of chitosan-based films related to their visual appearance (glossiness, transparency) may have a big impact on consumer acceptance (Vilela et al., 2017). The ability of packaging material to act as a barrier against the energy in the UV–vis light region is an added value in the context of photostability of specific food compounds (Duncan & Chang, 2012). Therefore, the optical properties of chitosan-based films were studied in terms of the light transmittance in the UV–vis light region, and the results are presented in Fig. 3.

Transmittance values in the UV range (≤400 nm) for the AE film were ranging from 33.6% to 68.7%, similarly like in the case of CH film (Fig. 3). The OE and HE films had values ranging from 0.0% to 32.2% and 38.4%, respectively. The addition of oak and hop extracts has caused a complete blockage of the UV light at the wavelengths up to ~330 nm (Fig. 3), probably due to the UV light absorption arising from the presence of extracts' components. The UV light barrier properties of tested chitosan-based films are in correlation with previously published findings (Kalaycıoğlu et al., 2017; Souza et al., 2017; Vilela et al., 2017).

Barrier capabilities in the visible wavelength range (> 400 nm) have increased after the incorporation of plant extracts (Fig. 3). The maximal transmittance (evaluated at the wavelengths higher than 650 nm) in blended films was reduced for ~10 percentage points compared to the control sample (i.e. from ~87% to ~77%). By comparison, the addition of 1% of the kenaf extract and ginger essential oil in two separate chitosan-based films caused similar maximal transmittance reduction (~10 percentage points) at the wavelengths higher than 650 nm (Souza et al., 2017). This can indicate a higher absorption capacity in the visible light region of the oak/hop extracts compared to the previously stated active components.

As the superior light absorption capacity of the OE/HE films is evident, it can be discussed that these films can be further selected for design and production of the packaging materials specifically tailored to block the most damaging light wavelengths, and therefore prevent the formation of toxic substances, off-odors and flavors, as well as loss of food color and photo-oxidation of lipids (Duncan & Chang, 2012; Tian, Decker, & Goddard, 2013).

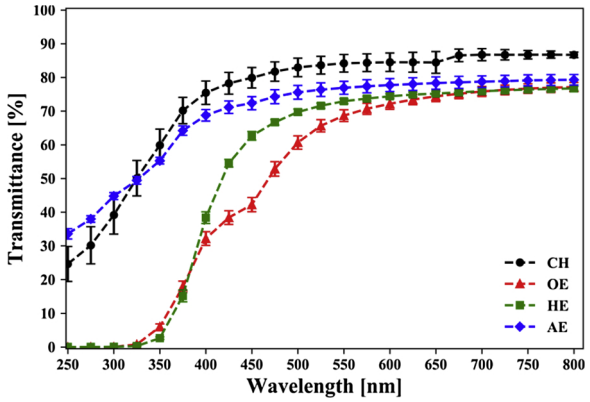

Fig. 3. The light transmittance of chitosan-based films in the UV–vis light region. The dashed lines are only for visual guidance.

3.5. Mechanical properties

Good mechanical properties of chitosan-based films are of high importance for their ability to provide a sufficient level of integrity during the post-process storage and handling of the food that is to be protected (Priyadarshi et al., 2018). In this context, *TS*, *EB*, and *YM* were studied in terms of resistance, pliability, and stiffness (Fig. 4).

The blended films displayed TS (from 5.5 MPa to 12.7 MPa) that was lower than in the case of CH film (Fig. 4a). Furthermore, blended films were able to deform plastically in higher extent than the control sample (from 14.0% to 31.0%) (Fig. 4b), pointing out a consistent behaviour concerning resistance and pliability. The evaluation of *YM* has revealed similar values for the CH/OE films (218.8 MPa/230.8 MPa), while the values for the HE/AE films (117.5 MPa/5.0 MPa) exhibited significantly reduced stiffness (Fig. 4c).

Generally speaking, the incorporation of plant extracts gave rise to decreasing of resistance (Fig. 4a) and stiffness (with an exception of the OE film; Fig. 4c), and increasing of pliability (Fig. 4b), as compared to the control sample. The variations of mechanical response suggest that the film structure softens and forms a more flexible structure with higher deformation values in the presence of a particular extract, which can be ascribed to the intermolecular interactions occurring between the extracts' components and chitosan molecules (Section 3.2). It can cause a decrease in the interactions that exist between chitosan chains, and hence cause discontinuities in the structure of blended films that ultimately lead to changes in mechanical response. In other words, at this concentration level the extracts appear to act as plasticizers by enhancing the molecular mobility of the polymer chains (Gursoy et al., 2018; Kaya, Ravikumar et al., 2018).

If we compare blended films among each other (Fig. 4a, b, c), it can be argued that higher resistance/stiffness and lower pliability of the OE film in regard to the HE film could be due to stronger crosslinking capacity of ellagitannins because they have a large number of potential interaction sites in regard to α-acids and β-acids. The AE film had the lowest resistance/stiffness and the highest pliability relative to the other two blended films. This can be ascribed to a possible presence of other components that affect mechanical properties since the extraction from the algal biomass is usually not so selective (Balboa et al., 2013). Another possible reason could be higher *MC* compared to the OE/HE films (Section 3.3), which is a parameter that can significantly affect mechanical properties (Aguirre-Loredo et al., 2016; Homez-Jara et al., 2018).

3.6. Total phenolic content

Natural antioxidants as fillers in active food packaging systems are important due to their role in the scavenging of oxidation inducers (Gómez-Estaca, López-de-Dicastillo, Hernández-Muñoz, Catalá, & Gavara, 2014; Tian et al., 2013). Therefore, *TPC* of chitosan-based films was evaluated and the results are presented in Fig. 5.

TPC in the AE film was 1.0 $mg_{GAE}\ g_{film}^{-1}$, similarly as in the case of the control sample (Fig. 5), whose low *TPC* might be due to the reaction between the FC reagent and $–NH_2$ groups from chitosan molecules (Bajić et al., 2019 and ref. therein). The reason for low *TPC* in the AE film could be either loss of the activity due to interactions between phenolic compounds and chitosan molecules or in poor efficiency of the extraction method (Balboa et al., 2013), i.e. a presumed presence of compounds that do not react with the FC reagent. A possible solution to this problem could be the application of non-aqueous solvents capable of extracting other antioxidant components.

On the contrary, *TPC* significantly increased in the OE (9.1 $mg_{GAE}\ g_{film}^{-1}$) and HE (2.5 $mg_{GAE}\ g_{film}^{-1}$) films, presumably as a consequence of the oak and hop extracts incorporation (Fig. 5). By comparison, the *TPC* values in chitosan-based films with incorporated 2.5% of propolis

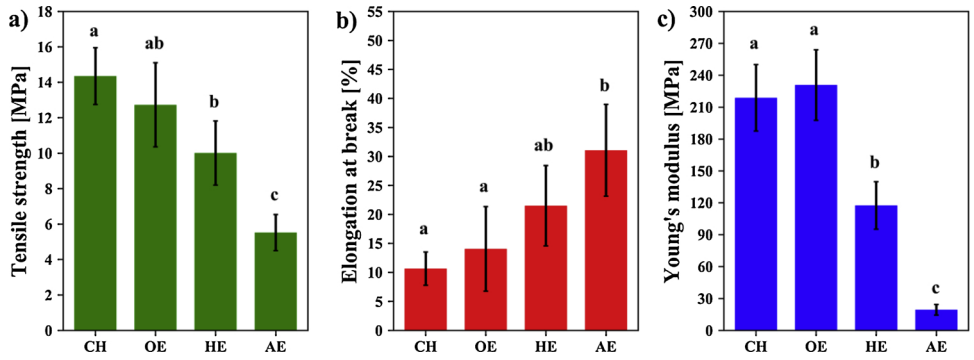

Fig. 4. Mechanical properties of chitosan-based films: a) tensile strength; b) elongation at break; c) Young's modulus. The samples with different letters have significantly different mean values ($p < 0.05$).

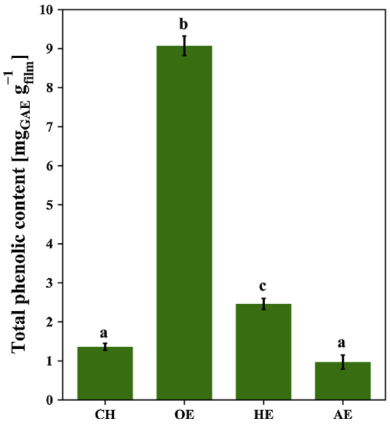

Fig. 5. Total phenolic content in chitosan-based films. The samples with different letters have significantly different mean values ($p < 0.05$).

extract (Siripatrawan & Vitchayakitti, 2016), 0.5% of maqui berry extract (Genskowsky et al., 2015), and 1.0% of *Eucalyptus globulus* essential oil (Hafsa et al., 2016), were approximately 4.2 $mg_{GAE}\ g_{film}^{-1}$, 4.7 $mg_{GAE}\ g_{film}^{-1}$, and 10.0 $mg_{GAE}\ g_{film}^{-1}$. On the other hand, a chitosan-based film containing the peanut skin extract had even up to 107.7 $mg_{GAE}\ g_{film}^{-1}$ (Serrano-León et al., 2018). High *TPC* value in chitosan-based films implies a high correlation with antioxidant activity (Hafsa et al., 2016), and therefore it can be very beneficial for the food preservation by preventing lipid oxidation, which presents the main cause of food spoilage after microbial contamination (Gómez-Estaca et al., 2014; Tian et al., 2013).

It has been previously shown that *TPC* in the hop extract-loaded films decreased for ~57% after 12 days of storage under ambient conditions due to oxidative degradation of the active components to humulinones and hulupones (Bajić et al., 2019 and ref. therein). It is also worth mentioning that possible oxidative degradation of the oak extract ellagitannins could lead to the appearance of the components such as tannins A and tannins B (Fujieda, Tanaka, Suwa, Koshimizu, & Kouno, 2008). Products of possible oxidative degradation of the algal extract components are very difficult to predict since the extract's qualitative composition has appeared to be quite complex (Appendix A, Fig. S3).

3.7. Antibacterial properties

Antibacterial activity against Gram-negative *E. coli* and Gram-positive *B. subtilis* was individually tested for each chitosan-based film, whereby the (non)existence of inhibition at the contact surface underneath the films, or inhibition zones around the films, were evaluated (Table 2). The accompanying pictures of the tested film samples are shown in Appendix A (Fig. S4).

Table 2
Antibacterial properties of chitosan-based films against *E. coli* and *B. subtilis*.

Microorganism	Film sample	*Contact inhibition	*Inhibition zone
E. coli	CH	+	–
	OE	+	–
	HE	+	–
	AE	+	–
B. subtilis	CH	+	–
	OE	+	+
	HE	+	+
	AE	+	–

* The signs" +" and" −" indicate existence and nonexistence of the contact inhibition underneath the film surfaces or inhibition zones around the films, respectively.

Both tested food-borne pathogens exhibited inhibition at the contact surface underneath the films, whereby the inhibition zone was observed in the case of *B. subtilis*, but only around the OE and HE films (Table 2; Appendix A, Fig. S4). Such a result indicates that the incorporation of oak and hop extracts enhanced the films' antimicrobial activity against *B. subtilis*, while *E. coli* was insensible. Besides, the existing inhibition zone was slightly bigger around the OE film compared to the HE film (Appendix A, Fig. S4), which could be a consequence of better water-solubility of the oak extract components relative to those stemming from the hop extract.

The antibacterial effect of the OE/HE films might be attributed to the main components from the oak and hop extracts, which are likely to release from the film matrix and diffuse into the agar medium. For instance, it has been shown that castalagin exhibits a strong activity against *Staphylococcus aureus*, but also against *E. coli* (Taguri, Tanaka, & Kouno, 2004). The reason for the absence of the inhibition zone around the OE film for *E. coli* could be in a relatively low extract concentration in the film. It could be expected that increasing the concentration of the oak extract could improve the antibacterial activity of the film, likewise in the case of hop extract, whose presumable mechanism of action is explained elsewhere (Bajić et al., 2019 and ref. therein).

4. Conclusions

The present study examines the possibility for utilization of renewable sources in the form of natural plant extracts as active components in chitosan-based films. Therefore, the films were separately incorporated by the extracts obtained from oak three, hop plant, and algae, and further evaluated and mutually compared.

The evaluation of obtained transparent, glossy, and smooth blended films has revealed that *MC*, *TSM*, and *EB* increased, while *TS*, *YM*, and *TPC* decreased as a consequence of the extract incorporation by following the pattern OE→HE→AE. This basically means that, among the blended films, the oak extract-containing film had the lowest amount of

water and total soluble matter alongside the highest phenolic content. This eventually led to the formation of material with favorable mechanical properties mirrored in the lowest pliability and the highest strength and stiffness in comparison to the other two blended films. Moreover, the OE film (alongside with the HE film) had advanced optical transmittance allowing a complete UV light blockage at the wavelengths below ~330 nm as well as satisfactory antibacterial activity against *B. subtilis*.

Based on the aforementioned facts, it can be concluded that the OE film is overcoming the performances of HE and AE films. Hence, it possesses high potential to be used as active food packaging material produced from natural-based, relatively cheap, and locally available components obtained from renewable sources. However, since it has been shown that higher concentrations of the extract can significantly alter the properties of the films (Bajić et al., 2019), further analyzes regarding the effect of the increased concentration of oak extract are highly recommended.

Acknowledgements

Financial support was provided by the BioApp project (a part of the Interreg V-A Italy-Slovenia 2014-2020 program) co-funded by the European Regional Development Fund and Slovenian Research Agency (research core funding No. P2-0152). Miša Mojca Cajnko, Ana Bjelić (National Institute of Chemistry, Ljubljana, Slovenia), Andrea Travan, Massimiliano Borgogna (Biopolife, Trieste, Italy), and Helena Jalšovec (Acies Bio, Ljubljana, Slovenia) are highly acknowledged for their generous help during the experimental work. The oak extract was a donation from the company Tanin Sevnica (Sevnica, Slovenia).

Appendix A. Supplementary data

Supplementary material related to this article can be found, in the online version, at doi:https://doi.org/10.1016/j.fpsl.2019.100365.

References

Aguirre-Loredo, R. Y., Rodríguez-Hernández, A. I., Morales-Sánchez, E., Gómez-Aldapa, C. A., & Velazquez, G. (2016). Effect of equilibrium moisture content on barrier, mechanical and thermal properties of chitosan films. *Food Chemistry, 196*, 560–566.

Akyuz, L., Kaya, M., Mujtaba, M., Ilk, S., Sargin, I., Salaberria, A. M., et al. (2018). Supplementing capsaicin with chitosan-based films enhanced the anti-quorum sensing, antimicrobial, antioxidant, transparency, elasticity and hydrophobicity. *International Journal of Biological Macromolecules, 115*, 438–446.

ASTM International (2002). *Designation D 882: "Standard test method for tensile properties of thin plastic sheeting"*. 10 p..

Augusto, A., Dias, J. R., Campos, M. J., Alves, N. M., Pedrosa, R., & Silva, S. F. J. (2018). Influence of *Codium tomentosum* extract in the properties of alginate and chitosan edible films. *Foods, 7*(4), 53.

Bajić, M., Jalšovec, H., Travan, A., Novak, U., & Likozar, B. (2019). Chitosan-based films with incorporated supercritical CO_2 hop extract: Structural, physicochemical, and antibacterial properties. *Carbohydrate Polymers, 219*, 261–268.

Balboa, E. M., Conde, E., Moure, A., Falqué, E., & Domínguez, H. (2013). *In vitro* antioxidant properties of crude extracts and compounds from brown algae. *Food Chemistry, 138*(2–3), 1764–1785.

Bi, F., Zhang, X., Bai, R., Liu, Y., Liu, J., & Liu, J. (2019). Preparation and characterization of antioxidant and antimicrobial packaging films based on chitosan and proanthocyanidins. *International Journal of Biological Macromolecules, 134*, 11–19.

Borić, M., Puliyalil, H., Novak, U., & Likozar, B. (2018). An intensified atmospheric plasma-based process for the isolation of the chitin biopolymer from waste crustacean biomass. *Green Chemistry, 20*(6), 1199–1204.

de Simón, B. F., Cadahía, E., Conde, E., & García-Vallejo, M. C. (1999). Ellagitannins in woods of spanish, french and american oaks. *Holzforschung, 53*(2), 147–150.

Duncan, S. E., & Chang, H.-H. (2012). Implications of light energy on food quality and packaging selection. In J. Henry (Vol. Ed.), *Advances in food and nutrition research: 67*, (pp. 25–73). Oxford: Elsevier Inc.

Elsabee, M. Z., & Abdou, E. S. (2013). Chitosan based edible films and coatings: A review. *Materials Science and Engineering C, 33*, 1819–1841.

Fujieda, M., Tanaka, T., Suwa, Y., Koshimizu, S., & Kouno, I. (2008). Isolation and structure of whiskey polyphenols produced by oxidation of oak wood ellagitannins. *Journal of Agricultural and Food Chemistry, 56*(16), 7305–7310.

García-Estévez, I., Alcalde-Eon, C., Le Grottaglie, L., Rivas-Gonzalo, J. C., & Escribano-Bailón, M. T. (2015). Understanding the ellagitannin extraction process from oak wood. *Tetrahedron, 71*(20), 3089–3094.

Genskowsky, E., Puente, L. A., Pérez-Álvarez, J. A., Fernandez-Lopez, J., Muñoz, L. A., & Viuda-Martos, M. (2015). Assessment of antibacterial and antioxidant properties of chitosan edible films incorporated with maqui berry (*Aristotelia chilensis*). *LWT - Food Science and Technology, 64*(2), 1057–1062.

Gómez-Estaca, J., López-de-Dicastillo, C., Hernández-Muñoz, P., Catalá, R., & Gavara, R. (2014). Advances in antioxidant active food packaging. *Trends in Food Science & Technology, 35*(1), 42–51.

Gursoy, M., Sargin, I., Mujtaba, M., Akyuz, B., Ilk, S., Akyuz, L., et al. (2018). False flax (*Camelina sativa*) seed oil as suitable ingredient for the enhancement of physicochemical and biological properties of chitosan films. *International Journal of Biological Macromolecules, 114*, 1224–1232.

Hafsa, J., ali Smach, M., Ben Khedher, M. R., Charfeddine, B., Limem, K., Majdoub, H., et al. (2016). Physical, antioxidant and antimicrobial properties of chitosan films containing *Eucalyptus globulus* essential oil. *LWT - Food Science and Technology, 68*, 356–364.

Homez-Jara, A., Daza, L. D., Aguirre, D. M., Muñoz, J. A., Solanilla, J. F., & Váquiro, H. A. (2018). Characterization of chitosan edible films obtained with various polymer concentrations and drying temperatures. *International Journal of Biological Macromolecules, 113*, 1233–1240.

Hosseinnejad, M., & Jafari, S. M. (2016). Evaluation of different factors affecting antimicrobial properties of chitosan. *International Journal of Biological Macromolecules, 85*, 467–475.

Kalaycıoğlu, Z., Torlak, E., Akın-Evingür, G., Özen, İ., & Erim, F. B. (2017). Antimicrobial and physical properties of chitosan films incorporated with turmeric extract. *International Journal of Biological Macromolecules, 101*, 882–888.

Kaya, M., Khadem, S., Cakmak, Y. S., Mujtaba, M., Ilk, S., Akyuz, L., et al. (2018). Antioxidative and antimicrobial edible chitosan films blended with stem, leaf and seed extracts of *Pistacia terebinthus* for active food packaging. *RSC Advances, 8*, 3941–3950.

Kaya, M., Ravikumar, P., Ilk, S., Mujtaba, M., Akyuz, L., Labidi, J., et al. (2018). Production and characterization of chitosan based edible films from *Berberis crataegina*'s fruit extract and seed oil. *Innovative Food Science & Emerging Technologies, 45*, 287–297.

Leceta, I., Guerrero, P., Cabezudo, S., & de la Caba, K. (2013). Environmental assessment of chitosan-based films. *Journal of Cleaner Production, 41*, 312–318.

Li, Y.-X., Wijesekara, I., Li, Y., & Kim, S. K. (2011). Phlorotannins as bioactive agents from brown algae. *Process Biochemistry, 46*(12), 2219–2224.

Lunkov, A. P., Ilyina, A. V., & Varlamov, V. P. (2018). Antioxidant, antimicrobial, and fungicidal properties of chitosan based films (review). *Applied Biochemistry and Microbiology, 54*(5), 444–454.

Mir, S. A., Dar, B. N., Wani, A. A., & Shah, M. A. (2018). Effect of plant extracts on the techno-functional properties of biodegradable packaging films. *Trends in Food Science & Technology, 80*, 141–154.

Muxika, A., Etxabide, A., Uranga, J., Guerrero, P., & de la Caba, K. (2017). Chitosan as a bioactive polymer: Processing, properties and applications. *International Journal of Biological Macromolecules, 105*, 1358–1368.

Mujtaba, M., Morsi, R. E., Kerch, G., Elsabee, M. Z., Kaya, M., Labidi, J., et al. (2019). Current advancements in chitosan-based film production for food technology; A review. *International Journal of Biological Macromolecules, 121*, 889–904.

O'Sullivan, A. M., O'Callaghan, Y. C., O'Grady, M. N., Queguineur, B., Hanniffy, D., Troy, D. J., et al. (2011). *In vitro* and cellular antioxidant activities of seaweed extracts prepared from five brown seaweeds harvested in spring from the west coast of Ireland. *Food Chemistry, 126*(3), 1064–1070.

Peng, Y., Wu, Y., & Li, Y. (2013). Development of tea extracts and chitosan composite films for active packaging materials. *International Journal of Biological Macromolecules, 59*, 282–289.

Priyadarshi, R., Sauraj, K. B., Deeba, F., Kulshreshtha, A., & Negi, Y. S. (2018). Chitosan films incorporated with Apricot (*Prunus armeniaca*) kernel essential oil as an active food packaging material. *Food Hydrocolloids, 85*, 158–166.

Serrano-León, J. S., Bergamaschi, K. B., Yoshida, C. M. P., Saldaña, E., Selani, M. M., Rios-Mera, J. D., et al. (2018). Chitosan active films containing agro-industrial residue extracts for shelf life extension of chicken restructured product. *Food Research International, 108*, 93–100.

Siripatrawan, U., & Harte, B. R. (2010). Physical properties and antioxidant activity of an active film from chitosan incorporated with green tea extract. *Food Hydrocolloids, 24*(8), 770–775.

Siripatrawan, U., & Vitchayakitti, W. (2016). Improving functional properties of chitosan films as active food packaging by incorporating with propolis. *Food Hydrocolloids, 61*, 695–702.

Soriano, A., Alañón, M. E., Alarcón, M., García-Ruíz, A., Díaz-Maroto, M. C., & Pérez-Coello, M. S. (2018). Oak wood extracts as natural antioxidants to increase shelf life of raw pork patties in modified atmosphere packaging. *Food Research International, 111*, 524–533.

Souza, V. G. L., Fernando, A. L., Pires, J. R. A., Rodrigues, P. F., Lopes, A. A. S., & Fernandes, F. M. B. (2017). Physical properties of chitosan films incorporated with natural antioxidants. *Industrial Crops and Products, 107*, 565–572.

Sun, L., Sun, J., Chen, L., Niu, P., Yang, X., & Guo, Y. (2017). Preparation and characterization of chitosan film incorporated with thinned young apple polyphenols as an active packaging material. *Carbohydrate Polymers, 163*, 81–91.

Taguri, T., Tanaka, T., & Kouno, I. (2004). Antimicrobial activity of 10 different plant polyphenols against bacteria causing food-borne disease. *Biological & Pharmaceutical Bulletin, 27*(12), 1965–1969.

Talari, A. C. S., Martinez, M. A. G., Movasaghi, Z., Rehman, S., & Rehman, I. U. (2017). Advances in Fourier transform infrared (FTIR) spectroscopy of biological tissues. *Applied Spectroscopy Reviews, 52*(5), 456–506.

Tian, F., Decker, E. A., & Goddard, J. M. (2013). Controlling lipid oxidation of food by

active packaging technologies. *Food & Function, 4*, 669–680.
Vilela, C., Pinto, R. J. B., Coelho, J., Domingues, M. R. M., Daina, S., Sadocco, P., et al. (2017). Bioactive chitosan/ellagic acid films with UV-light protection for active food packaging. *Food Hydrocolloids, 73*, 120–128.
Wang, L., Dong, Y., Men, H., Tong, J., & Zhou, J. (2013). Preparation and characterization of active films based on chitosan incorporated tea polyphenols. *Food Hydrocolloids, 32*(1), 35–41.
Younes, I., & Rinaudo, M. (2015). Chitin and chitosan preparation from marine sources. Structure, properties and applications. *Marine Drugs, 13*(3), 1133–1174.
Yuan, G., Chen, X., & Li, D. (2016). Chitosan films and coatings containing essential oils: The antioxidant and antimicrobial activity, and application in food systems. *Food Research International, 89*, 117–128.